

Reactive spark plasma sintering of $UAl_x + Al$ powder mixtures, prospects for manufacturing targets for ^{99}Mo production

Xavière Iltis^{1*}, Vincent Klosek¹, Kinam Kim², Jonghwan Kim², Yongjin Jeong²,
Stéphanie Lamy³, and Mathieu Pasturel³

¹ CEA, DES, IRESNE, DEC, Cadarache, F-13108 Saint-Paul-Lez-Durance, France

² Korea Atomic Energy Research Institute, 111 Daedeok-Daero 989 Beon-Gil, Daejeon, Yuseong-Gu 34057, Republic of Korea

³ Université de Rennes, CNRS, Institut des Sciences Chimiques de Rennes – UMR6226, F-35042 Rennes, France

Received: 25 August 2025 / Received in final form: 10 December 2025 / Accepted: 16 December 2025

Abstract. A U + 5 wt.% Al powder (written U-5Al), manufactured by centrifugal atomization, was used in this study to assess the feasibility of densifying $UAl_x + Al$ powder mixtures by Spark Plasma Sintering (SPS) and obtaining a final composition with a minimum content of UAl_2 that meets specifications of targets for ^{99}Mo production. The microstructure of the U-5Al powder was studied first and mainly consists of a mixture of UAl_2 primary dendrites and $\alpha-U$ phase. Three SPS conditions differing in terms of UAl_x/Al volume ratio and dwell time at 800 K were tested. The sintered discs were characterized by X-ray diffraction, optical microscopy, scanning electron microscopy and energy dispersive spectroscopy. A very quick transformation of the U-5Al particles into a mixture of aluminides ($UAl_2 + UAl_3 + UAl_4$, referred to UAl_x) was evidenced: only a few minutes were sufficient to transform the U-based particles into a mixture of aluminides containing about 80 wt.% of UAl_3 . According to these first tests, this new highly versatile manufacturing process could advantageously replace the conventional method of producing targets, subject to technical adjustments and parametric studies.

1 Introduction

^{99}Mo is used as a precursor of ^{99m}Tc , a radioisotope widely used in nuclear medicine. It is mainly produced in nuclear research reactors by irradiating dispersion-plate targets manufactured by the picture-frame method. This method consists in pressing a mixture of uranium-based and aluminium powders into a compact frame and covering it with aluminium alloy plates, through successive hot and cold rolling steps [1–3].

The most common U-bearing material for targets is a mixture of uranium aluminides (UAl_2 , UAl_3 , UAl_4) referred to UAl_x . Because of its congruent solidification, which allows synthesizing it in one step, and its relatively high U-content, UAl_2 is often chosen as the starting aluminide. Reactions between the U-based particles and the surrounding Al matrix occur during the manufacturing process and need to be optimized [4,5]. Indeed, unlike UAl_3 and UAl_4 , UAl_2 compound does not dissolve well in alkaline solutions commonly used for the extraction of ^{99}Mo [6,7]. It is thus preferable to minimize its amount in the final product [4,5]. Moreover, when UAl_4 is formed, this compound tends to crack and even evolve into powder [8–10], which is likely to affect the dimensions and

integrity of targets. For these reasons, UAl_3 is targeted as the main phase in the UAl_x mixture at the end of the manufacturing process.

Currently, worldwide efforts are pursued to replace high enriched uranium (HEU) by low enriched uranium (LEU, with ^{235}U content lower than 20%) in ^{99}Mo production targets. Materials with higher U density (such as U_3Si_2 or UO_2) are tested but their use necessitates to re-qualify the ^{99}Mo extraction process [11,12]. It is also possible to use pure U or U + Al alloy powders with low Al content, to obtain a suitable $UAl_x + Al$ mixture after reaction with the Al matrix [13,14]. This approach yielded encouraging results, for targets manufactured with atomized U-Al powders (with Al content ranging from 0 to 25 wt.%) using the picture-frame method, but a total of 7 hours at 823 K was the minimum required to eliminate the UAl_2 phase [15].

Spark plasma sintering (SPS) could be an alternative process for manufacturing $UAl_x + Al$ targets. It was already tested at laboratory scale to obtain composite $U_3Si_2 + Al$ fuel mini-plates [16]. On this basis, first SPS tests were carried out on $UAl_2 + Al$ powder mixtures to induce reactive sintering phenomena: after only a few minutes at temperatures ranging from 825 to 850 K, the UAl_2 phase was fully converted into a $UAl_3 + UAl_4$ mixture with a large amount of UAl_3 [17]. The present work aims to go

* e-mail: xaviere.iltis@cea.fr

Table 1. Main characteristics of the U-5Al/Al samples sintered by SPS in this study.

Sample designation	U-5Al/Al ratio (%vol)	Holding time at 800 K (min)
50/50-t0	50/50	0
50/50-t5	50/50	5
40/60-t10	40/60	10

further, by testing the reactivity of a UAl_x powder with 5 wt.% Al (written U-5Al), selected for its high U-content, in different sintering conditions at 800 K.

2 U-5Al powder characteristics

U-5Al powder was manufactured by the Korea Atomic Energy Research Institute (KAERI) by means of a centrifugal atomization method [18,19]. The density of this powder (measured by helium pycnometer) is $13.6 \pm 0.1 \text{ g cm}^{-3}$ and the median diameter of the particles (measured by laser granulometry) is about $60 \mu\text{m}$. It was characterized by X-ray diffraction (XRD), optical microscopy (OM), scanning electron microscopy (SEM) and energy dispersive spectroscopy (EDS), using the same instruments and methods as those described in [20].

X-ray diffraction revealed the presence of the following phases, which were quantified by Rietveld analysis using the FullProf software [21]: α -U ($62 \pm 5 \text{ wt.}\%$), UAl_2 ($35 \pm 5 \text{ wt.}\%$), UO_2 ($1 \pm 1 \text{ wt.}\%$) and UC ($2 \pm 1 \text{ wt.}\%$). The presence of some uranium oxide and carbide in atomized particles is consistent with previous studies on U_3Si_2 [20] and U-Mo [22]. SEM examinations coupled to EDS analyses of polished particle sections evidenced the presence of UAl_2 dendrites in a matrix containing α -U.

3 SPS process and testing grid

The SPS device used in this study was a HP-D-10 machine from FCT Systeme GmbH (Germany). Graphite dies and punches with 10 mm diameter were used. They were coated with a graphite foil (PapyexTM from Mersen) to facilitate unmoulding after sintering. Sintering experiments were performed under primary vacuum atmosphere. Temperatures were measured with a thermocouple placed in a hole drilled in the die wall. The heating and cooling rates were set at 100 K min^{-1} . The sintering temperature and pressure were set at 800 K and 76 MPa respectively. The dwell time at 800 K varied from 0 to 10 minutes.

Discs of 10 mm in diameter with a final thickness of about 0.5 mm were prepared as follows: a 325 mesh ($44 \mu\text{m}$) 99.7 wt.% aluminium powder supplied by STREM Chemicals was mixed manually and softly in an agate mortar with the U-5Al powder, in different volume ratios. This way, the U-5Al powder granulometry was not affected. To ensure a regular distribution of the powder bed in the die, it was manually spread using a spatula and then slowly pressed up to the desired pressure. The thermal cycle was then applied, the pressure being relaxed at the end of the cooling step.

Table 1 summarizes the main characteristics of the samples presented in this work. The first two ones have a 50/50 U-5Al/Al volume ratio, which corresponds to the maximum value currently used in the picture-frame process [3,23]. The theoretical U-loading of such a mixture (if 100% dense) is about $6.4 \text{ g}_\text{U} \text{ cm}^{-3}$. The third one has a 40/60 U-5Al/Al volume ratio, which equates to a U-loading of the order of $5.2 \text{ g}_\text{U} \text{ cm}^{-3}$.

4 Results

After sintering and demolding, graphite residues often remained stuck to the surface of the discs. Such residues were easily removed by a gentle mechanical polishing of their surface. Figures 1a, 1c and 1e correspond to optical images taken along a radius of such polished surfaces of the samples described in Table 1. On these images, aluminium appears in very light grey, transformed parts (by reaction with Al) of U-5Al particles are in medium gray, while untransformed kernels are darker (the dark color of untransformed kernels in U-5Al particles is due to the oxidation of the α -U phase that occurs in air after polishing). A few pores are also visible (in black). When increasing the dwell time at 800 K from 0 to 10 min, the number and size of untransformed parts in particles decrease, as also illustrated by the SEM images presented in Figures 1b, 1d and 1f. On this type of images taken in backscattered electron mode (BSE), Al appears in black, UAl_x regions are in medium grey and the α -U + UAl_2 remaining parts of the original U-5Al particles are in light grey (the UAl_2 dendrites being slightly discernible at this scale). There are practically no pores left (this was verified by increasing the contrast of the BSE images to observe the aluminium in dark grey and the pores in black).

Almost no aluminium is left around some of partly reacted U-5Al particles, such as those encircled by a red dotted line in Figure 1d. The availability of aluminium could therefore be a limiting factor for the transformation of all U-based particles into UAl_x (ideally UAl_2 -free). That is the reason why the third sample was prepared with a lower U-5Al/Al volume ratio of 40/60. This ratio was chosen because it is very close to that theoretically necessary to completely transform this mixture into UAl_3 . The holding time at 800 K was also increased up to 10 min. As shown by Figures 1e and 1f, the fraction of unreacted kernels is considerably smaller (but not zero), untransformed areas being located in places where U-5Al particles are closely packed, with less Al available.

Two ways of measuring the progress of the interdiffusion reaction between U-5Al and Al were tested: image

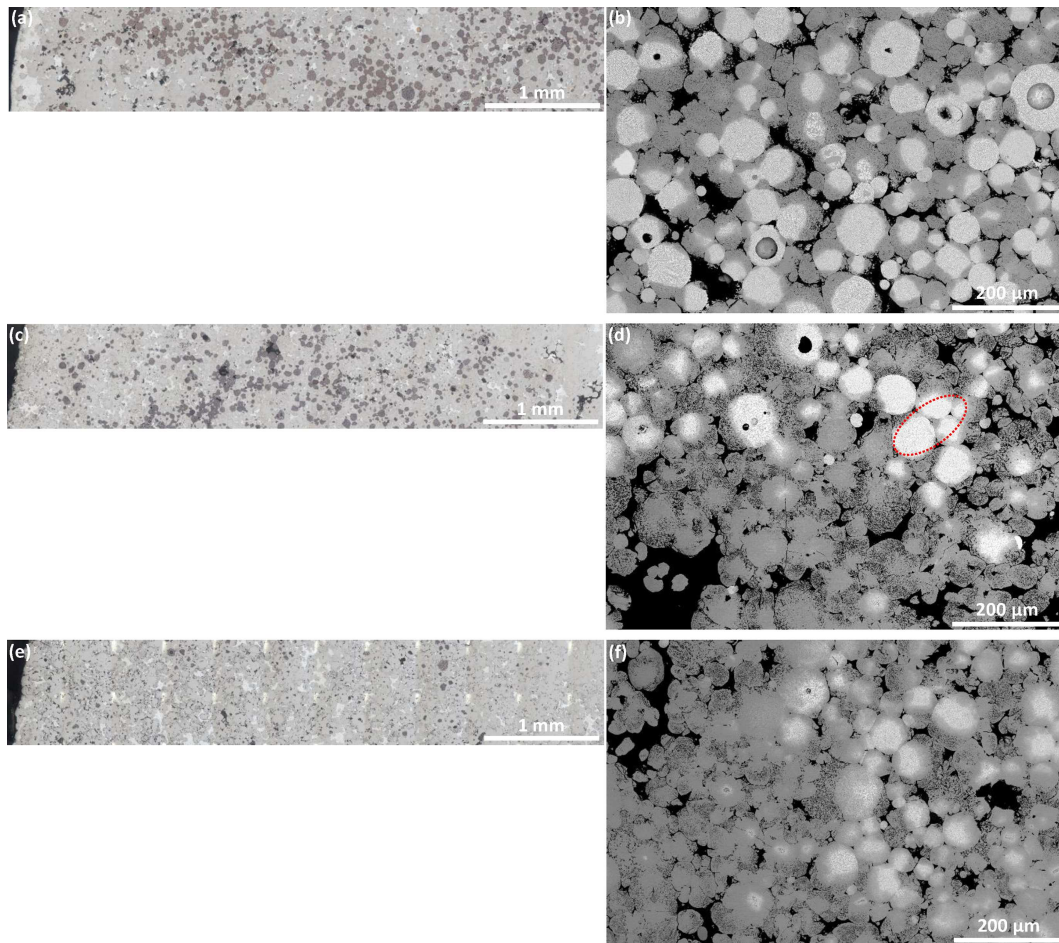


Fig. 1. Examination of U-5Al + Al samples after their spark plasma sintering, by optical microscopy (left) and by SEM in BSE mode (right). (a) (b) 50/50-t0 sample, (c) (d) 50/50-t5 sample, (e) (f) 40/60-t10 sample.

analysis (on optical and SEM images) and XRD. Image analysis failed to provide reliable results, mainly because the samples were not sufficiently homogeneous to be compared when considering a given polished section per sample. Moreover, threshold conditions were difficult to set to discriminate accurately the different phases (as also pointed out by Contorbria et al. [4]).

XRD analyses performed on polished surfaces of the pellets revealed no interaction between graphite and Al or U-5Al. As they also suffered from sample heterogeneity, only the mass ratios UAl_2/UAl_x , UAl_3/UAl_x and UAl_4/UAl_x were considered after quantification by the Rietveld method (the UAl_x content corresponding to the sum of the UAl_2 , UAl_3 and UAl_4 amounts). Figure 2 confirms the very rapid transformation of U-5Al particles into a mixture of aluminides. UAl_3 largely predominates and represents about 80 wt.% of the mixture, even after a 0 min holding time at 800 K. UAl_4 forms progressively with increasing holding time at this temperature and is present in approximately the same quantities in the 50/50-t5 and 40/60-t10 samples.

SEM examinations and EDS analyses confirmed the absence of interactions between graphite and Al or U-5Al. They showed how the U-5Al particles evolve when they

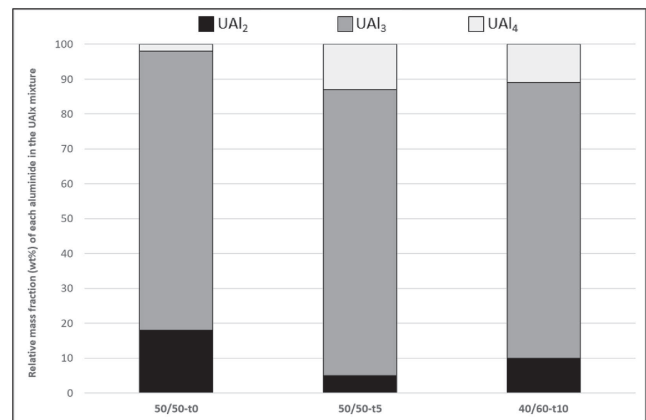


Fig. 2. Phase proportions in the U-5Al/Al sintered pellets, expressed in relative mass fractions of uranium aluminides, obtained from Rietveld analysis of XRD patterns of the 3 samples listed in Table 1.

react with Al. This evolution comprises two main stages observed in all the studied samples. Figure 3 illustrates the first stage. U-5Al particles have lost their round shape

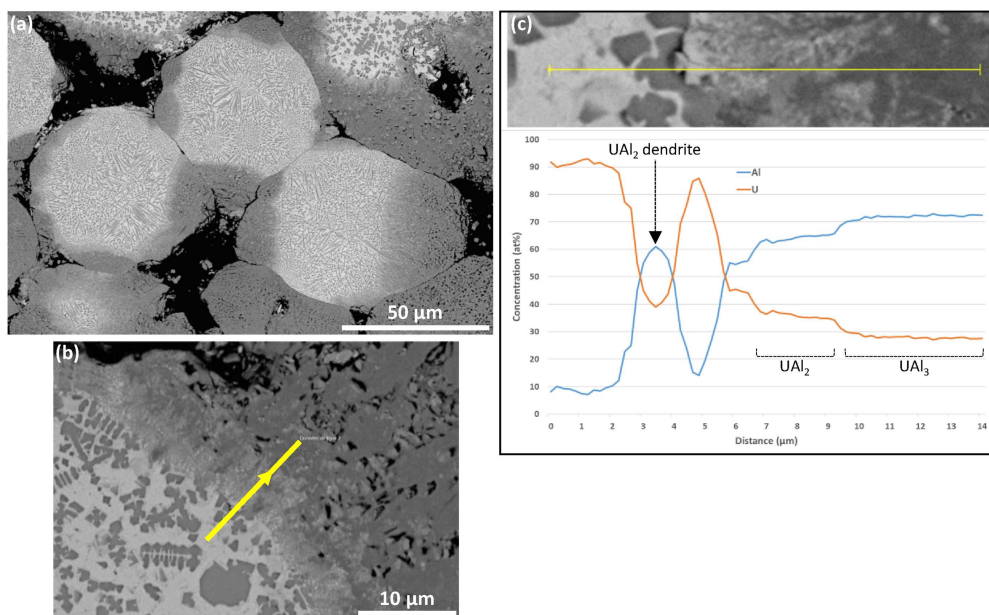


Fig. 3. (a) (b) SEM images (BSE mode) of a polished cross-section of the 50/50-t0 sample; (c) EDS linescan along the yellow line drawn on image (b).

and present irregular darker areas at their periphery with two main parts: an inner part, which appears dense, and a porous outer part. The EDS linescan presented in Figure 3c shows that they correspond respectively to areas where the UAl_2 and UAl_3 phases predominate. Note that, depending on the areas, a mixture of crystallites' of both aluminides can be found (as checked by punctual EDS analyses, which are not presented here).

Figure 4a shows how the microstructure evolves when most of the U-5Al particles are almost completely transformed into UAl_3 (except a few kernels, where primary UAl_2 dendrites are still visible). Their morphology is further and further far from their original round shape and they exhibit petal-shape protrusions with pores and cracks. In Figure 4b, SEM brightness and contrast settings were adjusted to reveal slight differences in grey levels within some transformed particles. The composition of lighter areas corresponds to that of UAl_3 (positions 1 and 2), whereas darker ones (positions 3, 4 and 5) correspond to UAl_4 (with a slight underestimation of the Al content, compared to the theoretical composition of these phases). This latter phase is often highly cracked, as observed in positions 4 and 5.

In agreement with XRD results, if few areas containing the UAl_4 phase were found in the 50/50-t0 sample, this phase was easily observed in the 50/50-t5 and 60/40-t10 samples, especially in areas where the Al fraction was locally higher.

5 Discussion

5.1 Interaction between U-5Al particles and Al in reactive SPS conditions

The U-5Al powder used in the present work contains α -U and UAl_2 phases. Around 800 K, studies performed on dif-

fusion couples point out a high reaction rate between α -U and Al to form UAl_3 [8,24,25] and a much slower reaction rate between UAl_2 and Al [10]. UAl_4 is formed after UAl_3 , at a slow rate [10,26]. Heat treatments performed on UAl_x +Al dispersions, and especially on UAl_2 +Al, broadly confirm these results, but with much slower kinetics, which could be due to the absence of applied pressure (unlike the case of diffusion couples) and/or the presence of an oxide layer on the surface of the particles acting as a diffusion barrier. On UAl_2 +Al mixtures, almost all UAl_2 was transformed into UAl_3 + UAl_4 after about 8 hours of holding at 813 K [4], while only 2.6 h were necessary at 853 K [5]. When using UAl_x atomized powders with 15 wt.% Al, in which the UAl_2 phase was the major constituent, 7 hours at 823 K were necessary to transform all this phase [15].

In SPS conditions, the reaction between UAl_2 and Al to form UAl_3 appears considerably accelerated compared to that observed in conventional heat treatment conditions. Indeed, the latter phase forms about 80 wt.% of the UAl_x mixture after only a few minutes at 800 K. UAl_4 also forms very quickly. Such an acceleration of solid state reactions has been observed in many materials and could be due to several phenomena: (i) a faster heating compared to a conventional one in a furnace as a result of the current passing through the powder compact [27] and the role of the current itself [28], (ii) a contribution from exothermic solid-state reactions that take place during sintering and lead to local temperature rise [27], (iii) enhanced diffusion kinetics by electromigration effects [29,30], (iv) pressure effects such as those observed in diffusion couples [24].

Despite the very fast formation of the UAl_3 phase, the UAl_4 fraction does not seem to increase significantly with the dwell time at 800 K (it stays around 10 wt.% of the UAl_x mixture for dwells of 5 and 10 min). This result could be due to insufficient local availability of Al and/or

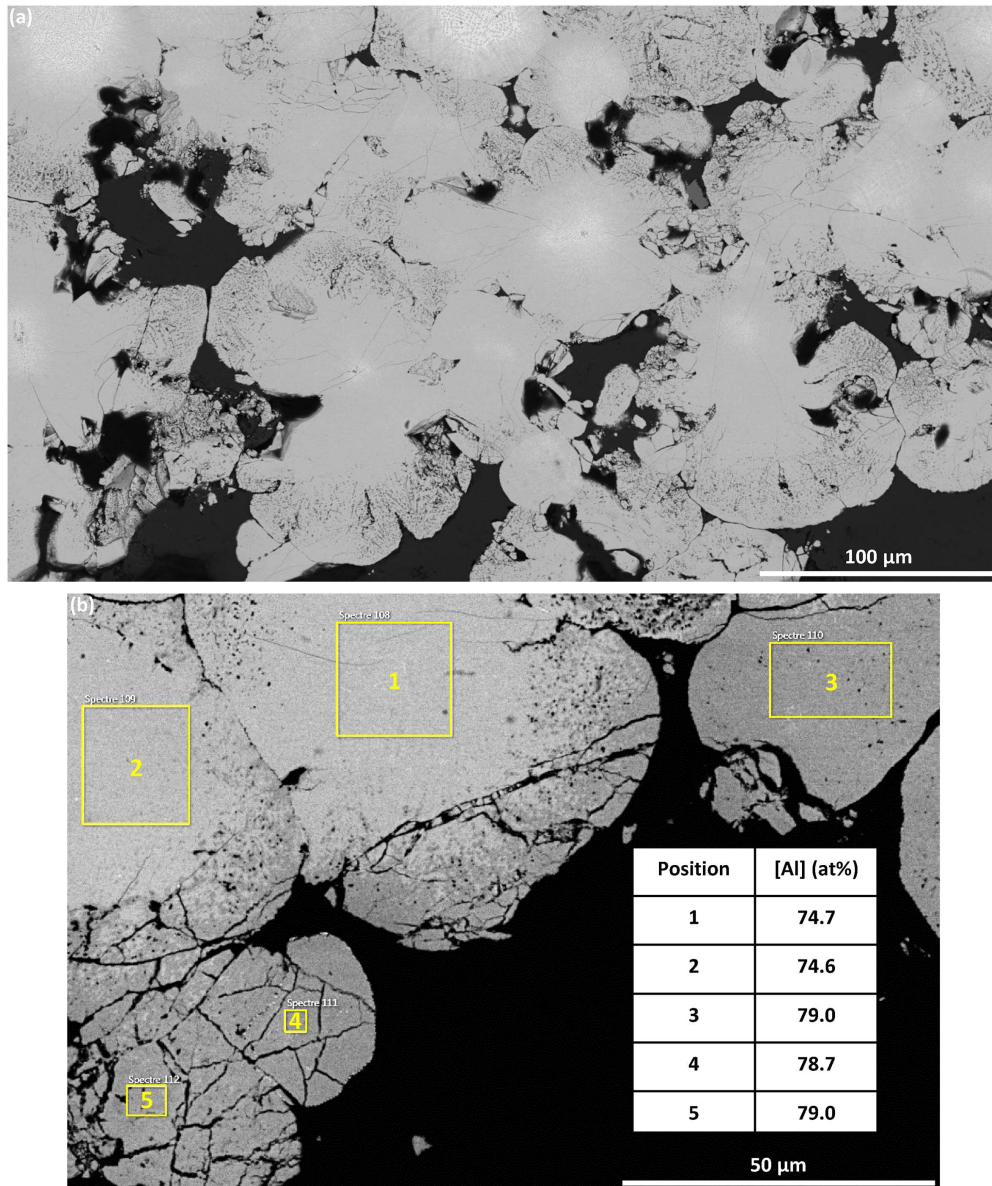


Fig. 4. SEM images (BSE mode) of a polished cross-section of the 50/50-t5 sample – (a) general view of an area where most of the U-5Al particles are transformed into UAl_3 , (b) enlarged view of particles containing the UAl_3 (positions 1 and 2) and UAl_4 phases (positions 3, 4 and 5). The Al content (at ± 2 at.%) at positions 1 to 5 was measured by EDS. The U content corresponds to the complement to 100%.

a stabilizing effect of the UAl_3 phase by Si (knowing that the U-5Al powder contains 0.04 wt.% Si), as reported by Boucher [9].

5.2 Ways to optimize the reactive SPS process

The experiments described in the present work were performed at laboratory scale for feasibility assessment purposes. The samples obtained showed heterogeneities in the distribution of UAl_x particles in the Al matrix which affected the local reactions. The first point of improvement would therefore be the homogeneity of the $UAl_x + Al$ powder mixture. The use of a TurbulaTM-type mixer (or

equivalent) to replace the manual mixing should be tested to ensure a gentle suitable blending of the two powders. The filling of the die by a regular layer of this powder mixture should also be improved by using dedicated tools and a particular attention should be paid to the risk of segregation between UAl_x and Al powder particles.

More generally, three groups of parameters should be studied and optimized to develop this new manufacturing process: the characteristics of the initial powder mixture, the sintering conditions and, finally, the cladding step of the sintered core (which was not investigated in the present work). Regarding the initial powder mixture, the composition of the U-based powder, its granulometry and its volume fraction must be adjusted so that the final

aluminide mixture is suitable for target dissolution operations. The amount of residual Al present after sintering must also be controlled to ensure satisfactory mechanical behavior and thermal properties of the targets during irradiation. The sintering cycle can be adapted in several ways in order to favor the desired composition of the final $UAl_x + Al$ mixture: by modifying the pressure value and application cycle, the heating and cooling rates, the temperature and holding time, etc. At last, the cladding operation could be carried out either by SPS (as proposed in [16]) or by other methods (e.g. rolling or high isostatic pressing).

Graphite residues could prevent a good cohesion between the sintered core and its cladding. A way to avoid this problem would be to sinter the $UAl_x + Al$ core and clad it in a single step. If the cladding was done separately, after sintering, slight mechanical polishing of the sintered disc before cladding would be necessary. This cladding step is likely to lead to changes in the characteristics of the sintered core. For this reason, it will be necessary to adjust the entire manufacturing process, in order to obtain a product that meets both irradiation and radioisotope extraction specifications. At the end, a change of geometry and scaling will be required to produce targets for ^{99}Mo production.

6 Conclusion

A U + 5 wt.% Al powder (written U-5Al), manufactured by centrifugal atomization, was used in this study to evaluate the feasibility of sintering $UAl_x + Al$ powder mixtures by SPS, as an alternative manufacturing method for targets used for ^{99}Mo production.

The microstructure of this powder was first studied. It mainly consists of a mixture of UAl_2 primary dendrites and α -U phase. Three SPS conditions were tested. They differ in terms of U-5Al volume ratio (40 and 50%) and dwell time (from 0 to 10 minutes) at 800 K. From X-ray diffraction, optical microscopy, scanning electron microscopy and energy dispersive spectroscopy characterizations, a very quick transformation of the U-5Al particles into a mixture of aluminides (UAl_x : $UAl_2 + UAl_3 + UAl_4$) has been evidenced. The progress of this transformation is closely linked to the local availability of Al and comprises two main steps with the successive appearance of the UAl_3 and UAl_4 phases. UAl_3 corresponds to about 80 wt.% of the UAl_x mixture, even after a 0 min holding time, and UAl_4 forms progressively in areas where enough Al is available Al as the holding time increases.

Technical adjustments are under progress and are required to improve the homogeneity of the U-5Al + Al mixture and the filling of the SPS machine die. Numerous parameters have also to be systematically studied and adjusted: mainly the U-5Al/Al (or UAl_x /Al, if different values are considered for x) volume ratio in the powder mixture, the heating rate, the temperature, the pressure and the dwell time for the sintering process. The cladding of the sintered core will also require numerous tests.

According to this first laboratory-scale study, after parametric tests and appropriate modifications to the

geometry and scale of the sintered objects, reactive SPS process could be a highly efficient target fabrication method for ^{99}Mo production.

Acknowledgments

Sébastien Legou worked as an intern on this subject and thanked for his contribution to the SPS experiments. The authors are also very grateful to Andrea Sanchez and Nicolas Tarisien for their help with sample preparation and characterization by XRD, optical microscopy, SEM and EDS.

Funding

This research did not receive any specific funding.

Conflicts of interest

The authors declare that they have no competing interests to report.

Data availability statement

Raw XRD data used to evaluate the kinetics of evolution of $UAl_x + Al$ mixtures (cf. Fig. 2) can be provided on request by the corresponding author.

Author contribution statement

X. Iltis: Investigation, Methodology, Writing – Original Draft Preparation. **V. Klosek**: Investigation, Methodology, Validation, Writing – Review & Editing. **K.N. Kim**: Supervision, Supply of U-based powder, Validation, Writing – Review & Editing. **J.H. Kim**: Supply of U-based powder, Writing – Review & Editing. **Y.J. Jeong**: Supply of U-based powder, Writing – Review & Editing. **S. Lamy**: Investigation, Methodology. **M. Pasturel**: Conceptualization, Supervision, Investigation, Methodology, Validation, Writing – Review & Editing.

Glossary of abbreviations

BSE	BackScattered Electron mode
EDS	Energy Dispersive Spectroscopy
HEU	High Enriched Uranium (^{235}U content > 20%)
LEU	Low Enriched Uranium (^{235}U content < 20%)
OM	Optical Microscopy
SEM	Scanning Electron Microscopy
SPS	Spark Plasma Sintering
XRD	X-Ray Diffraction
UAl_x	mixture of uranium aluminides ($UAl_2 + UAl_3 + UAl_4$)

References

1. A. Mushtak, Specifications and qualification of uranium/aluminium alloy plate target for the production of fission Molybdenum-99, Nucl. Eng. Des. **241**, 163 (2011), <https://doi.org/10.1016/j.nucengdes.2010.11.003>
2. K.L. Ali, A.A. Khan, A. Mushtak, F. Imtiaz, M.A. Ziai, A. Gulzar, M. Farooq, N. Hussain, N. Ahmed, S. Pervez, J.H. Zaidi, Development of low enriched uranium target plates by thermo-mechanical processing of UAl_2 -Al matrix for production of ^{99}Mo in Pakistan, Nucl. Eng. Des. **255**, 77 (2013), <https://doi.org/10.1016/j.nucengdes.2012.10.014>
3. M.A. Durazzo, G.L.C.R. Contorbia, E.F. Urano de Carvalho, Increasing productivity in the manufacture of UAl_2 -Al dispersion-plate targets for Mo-99 production, Progr. Nucl. Energy **140**, 103920 (2021), <https://doi.org/10.1016/j.pnucene.2021.103920>

4. G.L.C.R. Contorbria, M. Durazzo, E.F. Urano de Carvalho, H.G. Riella, Phase quantification in UAl_x -Al dispersion targets for Mo-99 production, *J. Nucl. Mater.* **509**, 465 (2018), <https://doi.org/10.1016/j.jnucmat.2018.07.029>
5. T.A.G. Restivo, G.L.C.R. Contorbria, E.F. Urano de Carvalho, M. Durazzo, Investigating solid-state reactions in UAl_2 -Al dispersions for Mo-99 target fabrication, *Appl. Radiat. Isot.* **220**, 111763 (2025), <https://doi.org/10.1016/j.apradiso.2025.111763>
6. H.J. Cols, P.R. Cristini, A.C. Manzini, Mo-99 from low-enriched uranium, in *RERTR International Meeting, Las Vegas, USA*, Oct. 1–6, 2000
7. C. Kohut, M. de la Fuente, P. Echenique, D. Podesta, P. Adelfang, Targets development of low enrichment for production of Mo^{99} for fission, in *RERTR International Meeting, Las Vegas, USA*, Oct. 1–6, 2000
8. L.S. DeLuca, H.T. Sumsion, Rate of Growth of Diffusion Layers in U-Al and U-AlSi Couples, 1957, Report KAPL-1747
9. R. Boucher, Etude des alliages aluminium-uranium. Application à la transformation à l'état solide $UAl_3 \rightarrow UAl_4$, *J. Nucl. Mater.* **1**, 13 (1959), [https://doi.org/10.1016/0022-3115\(59\)90007-8](https://doi.org/10.1016/0022-3115(59)90007-8)
10. C. Moussa, O. Tougait, B. Stepnik, Insights on the kinetics and mechanism behaviors of layer formation in UAl_2 -Al diffusion couple, in *RRFM Conference, Ljubljana, Slovenia*, 30 March–3 April, 2014
11. Non-HEU production technologies for Molybdenum-99 and Technetium-99m, IAEA Nuclear Energy Series n° NF-T-5.4, 2013
12. S.K. Lee, G.L. Beyer, J.S. Lee, Development of industrial-scale fission ^{99}Mo production process using low enriched uranium target, *Nucl. Eng. Technol.* **48**, 613 (2016), <https://doi.org/10.1016/j.net.2016.04.006>
13. H.J. Ryu, C.K. Kim, M. Sim, J.M. Park, J.H. Lee, Development of high-density U/Al dispersion plates for Mo-99 production using atomized uranium powder, *Nucl. Eng. Technol.* **45**, 979 (2013), <https://doi.org/10.5516/NET.07.2013.014>
14. H.J. Ryu, Y.J. Jeong, J.M. Nam, J.M. Park, Metallurgical considerations for the fabrication of low-enriched uranium dispersion targets with a high density for ^{99}Mo production, *J. Radioanal. Nucl. Chem.* **305**, 31 (2015), <https://doi.org/10.1007/s10967-014-3838-y>
15. T.W. Cho, K.N. Kim, S. Park, Y.J. Jeong, K.H. Lee, S.H. Kim, J.M. Park, Preliminary study of high-density LEU dispersion targets using an atomized uranium-aluminium powder, in *Trans. Korean Nucl. Soc. Spring Meeting, Jeju, Korea*, May 17–18, 2019
16. J. Havette, X. Iltis, H. Palancher, O. Fiquet, M. Pasturel, Short communication: Spark plasma sintering as an innovative process for nuclear fuel plate manufacturing, *J. Nucl. Mater.* **543**, 152541 (2021), <https://doi.org/10.1016/j.jnucmat.2020.152541>
17. X. Iltis, V. Klošek, A. Sanchez, N. Tarisien, S. Valance, S. Lamy, M. Pasturel, Reactive spark plasma sintering of $UAl_2 + Al$ powder mixtures, in *Proceedings of the RRFM Conference, Aix-en-Provence, France*, April 6–10, 2025
18. C.K. Kim, J.M. Park, H.J. Ryu, Use of a centrifugal atomization process in the development of research reactor fuel, *Nucl. Eng. Technol.* **39**, 617 (2007), <https://doi.org/10.5516/NET.2007.39.5.617>
19. S. Park, K.N. Kim, J.H. Kim, S. Kim, K.H. Lee, Y.J. Jeong, J.M. Park, Microstructural characterization of atomized UAl_x powder for high-density LEU dispersion target fabrication, in *Trans. Korean Nucl. Soc. Spring Meeting, Jeju, Korea*, May 16–18, 2018
20. X. Iltis, J. Havette, V. Klošek, C. Onofri, K.H. Lee, J.H. Kim, Y.J. Jeong, M. Pasturel, H. Palancher, Microstructural characterization of atomized U_3Si_2 powders with different silicon contents (7.4–7.8 wt.%), *J. Nucl. Mater.* **573**, 154141 (2023), <https://doi.org/10.1016/j.jnucmat.2022.154141>
21. J. Rodriguez-Carvajal, Recent advances in magnetic structure determination by neutron powder diffraction, *Phys. B: Condens. Matter.* **192**, 55 (1993), [https://doi.org/10.1016/0921-4526\(93\)90108-1](https://doi.org/10.1016/0921-4526(93)90108-1)
22. A. Bonnin, J.P. Wright, R. Tucoulou, H. Palancher, Impurity precipitation in atomized particles evidenced by nano X-ray diffraction computed tomography, *Appl. Phys. Lett.* **105**, 084103 (2014), <https://doi.org/10.1063/1.4894009>
23. M.M. Bretscher, J.E. Matos, Neutronic Performance of High-Density LEU Fuels in Water-Moderated and Water-Reflected Research Reactors, 1996, ANL/TD/RP-91011 Report, <https://doi.org/10.2172/373923>
24. A.D. Le Claire, I.J. Bear, The interdiffusion of uranium and aluminium, *J. Nucl. Energy* **2**, 229 (1956), [https://doi.org/10.1016/0891-3919\(55\)90039-5](https://doi.org/10.1016/0891-3919(55)90039-5)
25. L.S. Castelman, Layer growth during interdiffusion in the aluminium-uranium system, *J. Nucl. Mater.* **3**, 1 (1961), [https://doi.org/10.1016/0022-3115\(61\)90173-8](https://doi.org/10.1016/0022-3115(61)90173-8)
26. L. Kniznik, P.R. Alonso, P.H. Gargano, G.H. Rubiolo, Simulation of UAl_4 growth in an UAl_3/Al diffusion couple, *J. Nucl. Mater.* **414**, 309 (2011), <https://doi.org/10.1016/j.jnucmat.2011.04.056>
27. A.S. Mukasyan, A.S. Rogachev, D.O. Moskovskikh, Zh.Z. Yermekova, Reactive spark plasma sintering of exothermic systems: A critical review, *Ceram. Int.* **48**, 2988 (2022), <https://doi.org/10.1016/j.ceramint.2021.10.207>
28. Z.A. Munir, U. Anselmi-Tamburini, M. Ohyanagi, The effect of electric field and pressure on the synthesis and consolidation of materials: A review of the spark plasma sintering method, *J. Mater. Sci.* **41**, 763 (2006), <https://link.springer.com/article/10.1007/s10853-006-6555-2>
29. R. Li, T. Yuan, X. Liu, K. Zhou, Enhanced atomic diffusion of Fe-Al diffusion couple during spark plasma sintering, *Scr. Mater.* **110**, 105 (2016), [https://doi.org/10.1016/S1003-6326\(17\)60181-X](https://doi.org/10.1016/S1003-6326(17)60181-X)
30. S. Deng, T. Yuan, R. Li, M. Zang, S. Xie, M. Wang, L. Li, J. Yuan, Q. Weng, Influence of electric current on interdiffusion kinetics of W-Ti system during spark plasma sintering, *Int. J. Refract. Met. Hard Mater.* **75**, 184 (2018), <https://doi.org/10.1016/j.ijrmhm.2018.04.014>

Cite this article as: Xavière Iltis, Vincent Klošek, Kinam Kim, Jonghwan Kim, Yongjin Jeong, Stéphanie Lamy, Mathieu Pasturel. Reactive spark plasma sintering of $UAl_x + Al$ powder mixtures, prospects for manufacturing targets for ^{99}Mo production, *EPJ Nuclear Sci. Technol.* **12**, 7 (2026). <https://doi.org/10.1051/epjn/2025080>